Journal of Nuclear Medicine, published on May 26, 2016 as doi:10.2967/jnumed.116.174904

Quantitative Assessment of Breast Parenchymal Uptake in ^{18}F-FDG PET/CT: Correlation with Age, Background Parenchymal Enhancement, and Amount of Fibroglandular Tissue on MRI

Doris Leithner [1,2], Pascal A Baltzer[1], Heinrich F Magometschnigg [1], Georg J Wengert [1], Georgios Karanikas[3], Thomas H Helbich[1], Michael Weber[1], Wolfgang Wadsak[3], Katja Pinker[1]

[1] Department of Biomedical Imaging and Image-guided Therapy, Division of Molecular and Gender Imaging, Medical University of Vienna, Vienna, Austria

[2] Department of Diagnostic and Interventional Radiology, University Hospital Frankfurt, Frankfurt am Main, Germany

[3] Department of Biomedical Imaging and Image-guided Therapy, Division of Nuclear Medicine, Medical University of Vienna, Vienna, Austria

Running Title

Breast Parenchymal Uptake in 18F-FDG PET/CT

Key Words

18F-FDG PET/CT, Breast Parenchymal Uptake, Magnetic Resonance Imaging, Imaging Biomarker

Word count: 4858

Corresponding author:
Thomas H Helbich, MD, MBA, MSc
Medical University of Vienna/ Vienna General Hospital
Department of Biomedical Imaging and Image-guided Therapy

Division of Molecular and Gender Imaging
Waehringer Guertel 18-20
1090 Vienna
Austria
Email: thomas.helbich@meduniwien.ac.at

First author:
Doris Leithner
Medical University of Vienna/ Vienna General Hospital
Department of Biomedical Imaging and Image-guided Therapy
Division of Molecular and Gender Imaging
Waehringer Guertel 18-20
1090 Vienna
Austria
Email: doris.leithner@gmail.com

Quantitative Assessment of Breast Parenchymal Uptake in 18F-FDG PET/CT: Correlation with Age, Background Parenchymal Enhancement, and Amount of Fibroglandular Tissue on MRI

Abstract

Purpose

Background parenchymal enhancement (BPE), and the amount of fibroglandular tissue (FGT) assessed with magnetic resonance imaging (MRI) have been implicated as sensitive imaging biomarkers for breast cancer. The purpose of the study was to quantitatively assess the parenchymal uptake (BPU) on 18F-Fluorodeoxyglucose positron emission tomography/computed tomography (18F-FDG PET/CT) of the breast as another valuable imaging biomarker and examine its correlation with BPE, FGT, and age.

Methods

There were 129 patients with normal imaging findings in the one breast (BI-RADS 1) included in this IRB-approved study, whose cases were retrospectively analyzed. All patients underwent prone 18F-FDG PET/CT and 3T CE-MRI of the breast. In all patients, Reader 1 assessed BPU quantitatively using maximum standard uptake values. Two readers assessed FGT and BPE of the normal contralateral breast by subjective visual estimation, as recommended by BI-

RADS®. Reader 1 re-assessed all cases and repeated BPU measurements. Appropriate statistical tests were used to assess correlations of BPU, BPE, FGT, and age, as well as inter- and intra-reader agreement.

Results

BPU on 18F-FDG PET/CT varied between patients. The mean BPU SUVmax values ± SD for patients with minimal BPE were 1.57 ± SD 0.6, for mild BPE 1.93 ± SD 0.6, for moderate BPE 2.42 ± SD 0.5, and for marked BPE 1.45 ± SD 0.3. There were significant ($P<0.001$) moderate to strong correlations among BPU, BPE, and FGT. BPU is directly correlated with both BPE and FGT on MRI. Patient age showed a moderate to strong indirect correlation with all three imaging-derived tissue biomarkers. The coefficient of variation for quantitative BPU measurements with SUVmax was 5.6%, indicating a high reproducibility. Inter-reader and intra-reader agreement for BPE and FGT was almost perfect, with a Kappa value of 0.860 and 0.822, respectively.

Conclusion

The results of our study demonstrate that BPU varies between patients. BPU is directly correlated with both BPE and FGT on MRI, and BPU measurements are highly reproducible. Patient age showed strong inverse correlation with all three imaging-derived tissue biomarkers. These findings indicate that BPU may serve as a sensitive imaging biomarker for breast cancer prediction, prognosis, and risk assessment.

Introduction

Accurate risk assessment is pivotal for women at high risk for breast cancer to personalize risk-reduction interventions (*1*). In clinical practice, several risk-reduction strategies are being employed, ranging from lifestyle changes and chemo-prevention to invasive interventions, such as prophylactic mastectomy and salpingo-oophorectomy (*2-6*). Although these interventions are efficient in reducing cancer risk (*6,7*), they are associated with substantial side effects (*8,9*), and can negatively impact the quality of life (*10*). However, it currently remains uncertain which level of intervention is indicated for individual women (*11*), leading to potential over- and under-treatment. Therefore, methods to better determine the likelihood of response to risk-reduction interventions to better guide risk management decisions are urgently needed.

Magnetic resonance imaging (MRI) of the breast allows a three-dimensional assessment of both the anatomic and physiologic activity of breast tissue. In addition, MRI provides insight about the amount of fibroglandular breast tissue (FGT), as well as background parenchymal enhancement (BPE). Thus, FGT and

BPE are considered more sensitive predictive and prognostic imaging biomarkers than density assessment with mammography (*12-18*).

Similar to MRI, positron emission tomography (PET) using the radiotracer 18F-fluoro-deoxy-glucose (18F-FDG) provides insights into the physiologic activity of the normal breast parenchyma through the depiction of tissue glucose metabolism (*19-24*). This 18F-FDG uptake is defined as breast parenchymal uptake (BPU). Thus, it could be that BPU might also serve as an important imaging biomarker in breast cancer.

With the worldwide implementation of hybrid PET/MRI systems or dedicated breast PET systems, there is the potential to simultaneously assess and monitor these imaging biomarkers of breast cancer *(19,25,26*). To define the value of BPU, BPE, and FGT as imaging biomarkers for breast cancer and utilize these for better guidance of risk management decisions, information about their correlations and reproducibility is needed. However, to date, no such information exists. Therefore, the aim of this study was to quantitatively assess BPU on

18F-FDG PET/CT and examine its correlation with BPE and FGT on MRI and age.

Materials and Methods

The institutional review board approved this prospective, single-institution study and retrospective data analysis and all patients gave written, informed consent.

Patients

From 12/2009 to 04/2014, 172 consecutive patients were included in this study. Twenty-eight patients had to be excluded because of incomplete examinations or prior treatment. All patients fulfilled the following inclusion criteria and underwent 18F-FDG PET/CT and MRI: 18 years or older; not pregnant; not breastfeeding; suspicious finding at mammography or breast ultrasonography, i.e., asymmetric density, architectural distortion, breast mass, or microcalcifications (BI-RADS 0, further imaging warranted; 4, suspicious abnormality; 5, highly suggestive for malignancy); no previous treatment; and no contraindications for MRI or MRI contrast agents. In 30 patients, imaging revealed an abnormality in the contralateral breast (BI-RADS 2-5). All suspicious lesions were histopathologically verified by either image-guided or surgical biopsy. Of the 172 patients, 129 (age: 57.9 +/-3.9, range 18-87 years) who

presented with normal imaging findings on mammography, ultrasound, 18F-FDG PET/CT, and MRI in the contralateral breast (BI-RADS 1) were evaluated in this retrospective analysis.

A number of patients examined in this study have been previously analyzed in a different context (*19,22*).

Imaging

All patients underwent 18F-FDG PET/CT and MRI. Examinations were no longer than six days apart (mean 2.26; range 0-6; same day, n=57, 1 day, n=32, 2 days, n=11, 3 days, n=9, 4 days, n=12, 5 days, n=5, 6 days, n=1).

In all patients, a prone PET/CT dataset over the breasts was acquired using a combined PET/CT in-line system (Biograph 64 TruePoint® PET/CT system, Siemens, Erlangen, Germany), allowing the same patient geometry as with MRI. The whole-body PET/CT system is equipped with a high-resolution PET scanner and a 64-row-detector CT scanner. Patients fasted six hours before the injection of approximately 300 MBq 18F-FDG, depending on the patient's weight. Blood glucose levels were <150mg/dl (8.3 mmol/l) at the time

of tracer application. Up-take time was 60 minutes. No contrast agent was injected for the CT scan, which was used only for attenuation correction. PET images were reconstructed using the TrueX algorithm (Siemens, Erlangen, Germany) (*22*).

MRI imaging was performed in the prone position using a 3 T MRI (Tim Trio®, Siemens, Erlangen, Germany) and a four-channel breast coil (InVivo®, Orlando, FL, USA). In premenopausal patients, MRI was performed between the 7^{th} and 14^{th} day of the menstrual cycle to minimize hormonal influence on BPE (*27*).

The MRI protocol consisted of the following sequences:

A T2-weighted turbo spin echo sequence with fat suppression: TR/TE = 4800/9 msec; field of view 340mm; 48 slices at SI 3mm; flip angle 128°; matrix 384x512; time of acquisition: 2min 16sec.

A split dynamics, contrast-enhanced MRI protocol with the following parameters: T1-weighted Volume-Interpolated-Breathhold-Examination sequences (TR/TE 3.62/1.4ms; field of view 320mm; 72 slices; 1.7mm isotropic; matrix 192x192;

one average; 13.2sec per volume) and T1-weighted turbo fast-low-angle-shot-3D sequences with selective water-excitation (TR/TE 877/3.82ms; field of view 320mm; 96 slices; 1mm isotropic; matrix 320x134; one average; 2min) with a total time of acquisition of 15min 20sec.

A standard dose (0.1mmol/kg body-weight) of Gadotaremeglumine (Gd-DOTA; Dotarem®, Guerbet, France) was injected intravenously as a bolus using a power injector (Spectris Solaris EP®, Medrad, Pittsburgh, PA, USA) at 4 ml/s with a saline flush after injection. Total MRI examination time was approximately 18 minutes.

Data analysis

18F-FDG PET/CT

After image reconstruction, a three-dimensional region of interest (ROI) was carefully drawn on the contralateral normal breast around the glandular breast tissue, as determined by visual inspection on the consequent 4-6 PET/CT scan slices by a breast radiologist under the supervision of a nuclear medicine physician. The nipple and areola area were excluded from ROI placement. From

these ROIs, the maximum standardized uptake value (SUVmax) was calculated. In all patients, BPU SUVmax measurements were repeated by Reader 1 to assess reproducibility.

MRI

In all patients, FGT and BPE of the normal contralateral breast were qualitatively assessed by two independent readers using the revised American College of Radiology (ACR) BI-RADS® classification (*28*). For calculation of intra-reader agreement, Reader 1 re-assessed all cases. As recommended by ACR BI-RADS®, FGT and BPE were assessed by visual subjective estimation for each MRI study. FGT was classified as ACR a – for almost entirely fatty breasts, as ACR b – for breasts with scattered fibroglandular tissue, as ACR c – for breasts with heterogeneous fibroglandular tissue, and as ACR d – for breasts with extreme fibroglandular tissue content. BPE was graded as minimal, mild, moderate, or marked, based on post-contrast images approximately 90 seconds after contrast media injection.

Statistical analysis

Statistical analysis was performed using IBM SPSS Statistics version 22.0. Metric data, such as BPU SUVmax values and age, are described using means +/- standard deviation, and nominal and ordinal data are presented using absolute frequencies and percentages. In order to compare average age and BPU for different BPE and FGT grades, one-way analyses of variance and post-hoc Tukey's range tests were calculated. The Pearson correlation coefficient (r) was assessed for the correlation between age and BPU, and Spearman rank correlations (rho) for the correlation between BPE and FGT. For FGT and BPE, Cohen's Kappa was used, and, for BPU, the coefficient of variance was used to calculate inter- and intra-reader agreement. A p-value □ 0.05 was considered a significant result. A correlation coefficient matrix showing numerical, color- and size-coded Pearson correlation coefficients for BPU SUVmax values in 18F-FDG PET/CT, BPE and FGT on MRI and age for both readers and reassessment of BPU SUVmax values by reader 1 was calculated. 0 indicated no correlation, 0-3 indicated a weak correlation, 3-5 indicated a

moderate correlation, 5-7 indicated a strong correlation, and >7 indicated an excellent correlation.

Results

Mean, standard deviation (SD), minimum, and maximum BPU SUVmax values on 18F-FDG PET/CT for all patients were 1.81, 0.61, 0.88, and 4.55, respectively. The mean BPU SUVmax values ± SD and 25^{th} and 75^{th} percentile for patients with minimal BPE were 1.57 ± SD 0.6 [1.27-1.88], for mild BPE 1.93 ± SD 0.6 [1.44-2.31], for moderate BPE 2.42 ± SD 0.5 [2.06-2.85], and for marked BPE 1.45 ± SD 0.3 [1.09-.]. Thus, BPU on 18F-FDG PET/CT varied between patients.

BPE was minimal in 58 (44.96%), mild in 54 (41.86%), moderate in 14 (10.85%), and marked in 3 (2.33%) patients. FGT was classified as ACR a in 33, ACR b in 59, ACR c in 27 and ACR d in 10 patients. The mean BPU SUVmax values ± SD and 25^{th} and 75^{th} percentile for patients with FGT-ACR a were 1.54 ± SD 0.5 [1.15-1.89], for FGT-ACR b 1.75 ± SD 0.5 [1.36-2.16], for FGT-ACR c 2.01 ± SD 0.75 [1.48-2.44], and for FGT-ACR d 2.29 ± SD 0.66 [1.79-2.54]. Detailed results of ACR classification for BPE and FGT by both readers and reading rounds (r1_1; r1_2,; r2) are summarized in Table 1.

Correlations of BPU, BPE, FGT, and age for both readers are summarized in the correlation coefficient matrix showing numerical, color-, and size-coded Pearson correlation coefficients (Fig.1). Correlation coefficients ranged between moderate, i.e., 0.3-0.5 (BPU with age, BPE with FGT; BPE with FGT) and strong, i.e., 0.5-0.7 (age with BPU, BPE, and FGT).

BPU showed a significant moderate direct correlation with BPE ($p<0.001$, rho=0.492), indicating that patients with greater levels of BPE present with greater BPU SUVmax values (Figs. 2 and 3). BPU showed a significant moderate direct correlation with FGT ($p<0.001$, rho=0.370), indicating that patients with a larger amount of FGT present with greater BPU SUVmax values (Figs. 2 and 3).

All three imaging derived tissue biomarkers, i.e., BPU (r=0.386), BPE (rho=-0.498), and FGT (rho=-0.631), showed a significant indirect correlation with age ($p<0.001$).

When moderate and marked BPE were grouped together and considered as a “category of greater levels of BPE”, results were not different. Mean BPU

values and SD for “category of greater levels of BPE” was 2.25 ± SD 0.6. Correlations of BPU, BPE, FGT, and age for this grouped analysis for both readers are summarized in the correlation coefficient matrix showing numerical, color-, and size-coded Pearson correlation coefficients (Supplemental Figure 1). Correlation coefficients ranged between moderate, i.e., 0.3-0.5 (BPE with FGT) and strong, i.e., 0.5-0.7 (age with BPE). BPU showed a significant moderate direct correlation with BPE ($p<0.001$, rho=0.422). FGT showed a significant moderate direct correlation with BPE ($p<0.001$, rho=0.474). BPE (rho=-0.498) showed a significant indirect correlation with age ($p<0.001$).

The coefficient of variance for quantitative BPU measurements with SUVmax was 5.6%, indicating a high reproducibility. Inter- and intra-reader agreement for BPE was almost perfect with Kappa values of 0.860 and 0.822, respectively. Inter- and intra-reader agreement for FGT was also almost perfect, with Kappa values of 0.839 and 0.931 respectively.

Discussion

PET imaging has been implemented worldwide in oncologic imaging and is used in breast assessment, with promising results (*19,22,29,30*). BPE and FGT on MRI have been implicated as sensitive predictive and prognostic imaging biomarkers in breast cancer (*12-15,17,31*). The investigation of BPU as another potential sensitive and also quantifiable imaging biomarker for breast cancer prediction, prognosis, and risk assessment is, therefore, of considerable interest. To fully elucidate the value of BPU, BPE, and FGT as imaging biomarkers for breast cancer, information about their correlations and reproducibility are needed.

The results of our study demonstrate that BPU, which is the degree of 18F-FDG uptake in the glandular tissues of the normal breast, varies between patients. BPU was directly correlated with both MRI-derived BPE and FGT. Patient age showed a moderate to strong indirect correlation with all three imaging-derived tissue biomarkers. BPU measurements were highly reproducible, and there was almost perfect inter- and intra-reader agreement for both BPE

and FGT with MRI. These findings indicate that BPU may serve as a sensitive predictive and prognostic imaging biomarker for breast cancer prediction, prognosis, and risk assessment.

To our knowledge, this is the first study to examine the correlation of BPU on 18F-FDG PET/CT with BPE and FGT on MRI. We identified a significant direct correlation between BPU and BPE and FGT, which suggests that BPU could also be used as an imaging biomarker for risk assessment, hormonal replacement therapy, or chemo-prevention. Just as the imaging biomarkers BPE and FGT on MRI, BPU can be assessed non-invasively, but a definite benefit of BPU compared to BPE and FGT is that it can be assessed quantitatively and is highly reproducible, which is a prerequisite for a stable and clinically relevant imaging biomarker (*32,33*).

To date, the correlation of 18F-FDG radiotracer uptake in normal breast parenchyma with BPE has been investigated using solely 18F-FDG positron emission mammography (18F-FDG PEM). In this single retrospective study, Koo et al. assessed the correlation of BPU on 18F-FDG PEM, BPE on CE-MRI, and

mammographic breast density (*34*). Although mean BPU increased from minimal to marked BPE, there was considerable overlap, especially for women with minimal and mild BPE, and mean BPU was not an independent predictor of BPU on PEM. In contrast, in the current study, we found a direct correlation between BPU and BPE. The divergent results might be explained by the fact that, in the study by Koo et al., there was a small sample size, especially for moderate (n=5) and marked BPE (n=5), which may have led to underpowered statistical analyses. Moreover, in contrast to the current study, BPU was assessed using a two-dimensional imaging modality, i.e., 18F-FDG PEM, which could have influenced the results, and thus, limits comparability. In addition, MRIs were not scheduled according to the menstrual cycle, and there is no information on the time-interval between PEM and MRI, which potentially might act as another confounding factor.

Currently, no information exists on the correlation of BPU and FGT on MRI, which is a newly introduced BI-RADS descriptor in the ACR MRI BI-RADS® lexicon. In this first study to examine the correlations between BPU and

FGT, we found a direct correlation. This is in agreement with studies that have investigated the correlation of BPU on 18F-FDG PET or PEM and mammographic breast density, which is the equivalent of FGT on MRI. *(34-37)*. These results further underline the potential of BPU as a valuable imaging biomarker in breast cancer.

An increased mammographic breast density, which is the equivalent of FGT on MRI, has been demonstrated to decrease with age. Similar to mammographic breast density, all three tissue-derived imaging biomarkers in our study also showed an indirect correlation with patients' age. To date, results regarding the correlation of BPU with age are scarce and divergent. Similar to our results, Mavi et al., Zytoon et al., and Koo et al. demonstrated that 18F-FDG uptake significantly decreases as age increases (*29,34,36,37*). Only one study by Vranjesevic et al. found no significant correlation (*35*).

BPE and FGT also showed a negative correlation with age, which is in agreement with previously published data that investigated BPE and mammographic breast density (*38,39,40*).

A clinically relevant imaging biomarker must be stable and reproducible. In this study, we demonstrated that BPU provides those qualities, as quantitative BPU measurements are highly reproducible. Our findings are in accordance with Vranjesevic et al. and Mavi et al., who found good agreement between quantitative BPU measurements when measured by two observers independently (*35,37*). In this study, there was almost perfect inter- and intra-reader agreement for both BPE and FGT in MRI. Previous studies reported a good agreement for BPE classification when performed by trained readers (*17,41*), but yielded more variability when read by inexperienced readers, thus somewhat limiting its ability as a stable imaging biomarker. The excellent results in the current study can be explained by the fact that both readers were experienced with breast density assessment and MRI. Currently, there is no data on inter- and intra-observer agreement for FGT, as this parameter has only recently been introduced into the ACR MRI BI-RADS lexicon. In contrast to mammographic breast density (*42*), where there is considerable variability, inter- and intra-reader agreement was almost perfect for FGT. Similar to the excellent results for BPE, this is

most likely due to the fact that our readers had vast experience with breast density assessment and MRI.

The current study has some limitations. A limitation of our study is the small number of patients with marked BPE. However, this reflects the normal distribution of BPE in the population. Additioanlly, we performed a grouped analysis for patients with greater levels of BPE, i.e moderate and marked, which yielded similar results. In this study, in contrast to BPU, BPE and FGT were assessed qualitatively. However, currently, the ACR BI-RADS lexicon does not recommend quantitative assessment of BPE and FGT, but there was excellent intra- and inter-reader agreement for BPE and FGT. Therefore, the approach in this study seems to be justified. In this study, not all PET/CT and MRI examinations were performed on the same day (range 0-6), which potentially might have had an impact on BPE in a few cases due to the changes in BPE with the menstrual cycle. However, in the majority of cases, the interval between examinations was short (mean 2.26 days), and thus, relevant changes in BPE seem unlikely.

In conclusion, the results of our study demonstrate that BPU varies between patients. BPU is directly correlated with both BPE and FGT on MRI. Patient age shows a strong inverse correlation with all three imaging-derived tissue biomarkers. BPU measurements are highly reproducible, with almost perfect inter- and intra-reader agreement for both BPE and FGT with MRI. These findings indicate that BPU may serve as a sensitive imaging biomarker for breast cancer prediction, prognosis, and risk assessment.

References

1. Lee K, Rossi C. Risk Assessment, Genetic Counseling, and Genetic Testing for BRCA-Related Cancer in Women. *Am Fam Physician.* 2015;91:119-120.

2. Lahart IM, Metsios GS, Nevill AM, Carmichael AR. Physical activity, risk of death and recurrence in breast cancer survivors: A systematic review and meta-analysis of epidemiological studies. *Acta Oncol.* 2015;54:635-654.

3. Morrow M, Jordan VC. Tamoxifen for the prevention of breast cancer in the high-risk woman. *Ann Surg Oncol.* 2000;7:67-71.

4. Cuzick J, Forbes JF, Sestak I, et al. Long-term results of tamoxifen prophylaxis for breast cancer--96-month follow-up of the randomized IBIS-I trial. *J Natl Cancer Inst.* 2007;99:272-282.

5. Burke EE, Portschy PR, Tuttle TM. Prophylactic mastectomy: who needs it, when and why. *J Surg Oncol.* 2015;111:91-95.

6. Advani P, Moreno-Aspitia A. Current strategies for the prevention of breast cancer. *Breast Cancer (Dove Med Press).* 2014;6:59-71.

7. Lostumbo L, Carbine NE, Wallace J. Prophylactic mastectomy for the prevention of breast cancer. *Cochrane Database Syst Rev.* 2010:CD002748.

8. Kinsinger LS, Harris R, Woolf SH, Sox HC, Lohr KN. Chemoprevention of breast cancer: a summary of the evidence for the U.S. Preventive Services Task Force. *Annals of internal medicine.* 2002;137:59-69.

9. Parker WH. Bilateral oophorectomy versus ovarian conservation: effects on long-term women's health. *J Minim Invasive Gynecol.* 2010;17:161-166.

10. Brandberg Y, Arver B, Johansson H, Wickman M, Sandelin K, Liljegren A. Less correspondence between expectations before and cosmetic results after risk-reducing mastectomy in women who are mutation carriers: a prospective study. *Eur J Surg Oncol.* 2012;38:38-43.

11. Morris JL, Gordon OK. *Positive results: making the best decisions when you're at high risk for breast or ovarian cancer.* . Amherst, NY: Prometheus Books; 2010.

12. King V, Brooks JD, Bernstein JL, Reiner AS, Pike MC, Morris EA. Background parenchymal enhancement at breast MR imaging and breast cancer risk. *Radiology.* 2011;260:50-60.

13. Dontchos BN, Rahbar H, Partridge SC, et al. Are Qualitative Assessments of Background Parenchymal Enhancement, Amount of Fibroglandular Tissue on MR Images, and Mammographic Density Associated with Breast Cancer Risk? *Radiology.* 2015;276:371-380.

14. Kim MY, Cho N, Koo HR, et al. Predicting local recurrence following breast-conserving treatment: parenchymal signal enhancement ratio (SER) around the tumor on preoperative MRI. *Acta Radiol.* 2013;54:731-738.

15. Kim SA, Cho N, Ryu EB, et al. Background parenchymal signal enhancement ratio at preoperative MR imaging: association with

subsequent local recurrence in patients with ductal carcinoma in situ after breast conservation surgery. *Radiology.* 2014;270:699-707.

16. McCormack VA, dos Santos Silva I. Breast density and parenchymal patterns as markers of breast cancer risk: a meta-analysis. *Cancer Epidemiol Biomarkers Prev.* 2006;15:1159-1169.

17. Preibsch H, Wanner L, Bahrs SD, et al. Background parenchymal enhancement in breast MRI before and after neoadjuvant chemotherapy: correlation with tumour response. *European radiology.* 2015.

18. Wengert GJ, Helbich TH, Vogl WD, et al. Introduction of an automated user-independent quantitative volumetric magnetic resonance imaging breast density measurement system using the Dixon sequence: comparison with mammographic breast density assessment. *Invest Radiol.* 2015;50:73-80.

19. Pinker K, Bogner W, Baltzer P, et al. Improved differentiation of benign and malignant breast tumors with multiparametric 18fluorodeoxyglucose

positron emission tomography magnetic resonance imaging: a feasibility study. *Clin Cancer Res.* 2014;20:3540-3549.

20. Avril N, Adler LP. F-18 fluorodeoxyglucose-positron emission tomography imaging for primary breast cancer and loco-regional staging. *Radiol Clin North Am.* 2007;45:645-657, vi.

21. Miles KA, Williams RE. Warburg revisited: imaging tumour blood flow and metabolism. *Cancer imaging : the official publication of the International Cancer Imaging Society.* 2008;8:81-86.

22. Magometschnigg HF, Baltzer PA, Fueger B, et al. Diagnostic accuracy of (18)F-FDG PET/CT compared with that of contrast-enhanced MRI of the breast at 3 T. *European journal of nuclear medicine and molecular imaging.* 2015;42:1656-1665.

23. Koolen BB, van der Leij F, Vogel WV, et al. Accuracy of 18F-FDG PET/CT for primary tumor visualization and staging in T1 breast cancer. *Acta oncologica.* 2014;53:50-57.

24. Moy L, Noz ME, Maguire GQ, Jr., et al. Prone mammoPET acquisition improves the ability to fuse MRI and PET breast scans. *Clin Nucl Med.* 2007;32:194-198.

25. Koolen BB, Vidal-Sicart S, Benlloch Baviera JM, Valdes Olmos RA. Evaluating heterogeneity of primary tumor (18)F-FDG uptake in breast cancer with a dedicated breast PET (MAMMI): a feasibility study based on correlation with PET/CT. *Nucl Med Commun.* 2014;35:446-452.

26. Fraum TJ, Fowler KJ, McConathy J. PET/MRI:: Emerging Clinical Applications in Oncology. *Acad Radiol.* 2016;23:220-236.

27. Mann RM, Balleyguier C, Baltzer PA, et al. Breast MRI: EUSOBI recommendations for women's information. *European radiology.* 2015;25:3669-3678.

28. *BI-RADS® Atlas*. 5th Edition ed2013.

29. Zytoon AA, Murakami K, El-Kholy MR, El-Shorbagy E. Dual time point FDG-PET/CT imaging... Potential tool for diagnosis of breast cancer. *Clin Radiol.* 2008;63:1213-1227.

30. Kalles V, Zografos GC, Provatopoulou X, Koulocheri D, Gounaris A. The current status of positron emission mammography in breast cancer diagnosis. *Breast cancer.* 2013;20:123-130.

31. Park VY, Kim EK, Kim MJ, Yoon JH, Moon HJ. Breast parenchymal signal enhancement ratio at preoperative magnetic resonance imaging: association with early recurrence in triple-negative breast cancer patients. *Acta Radiol.* 2015.

32. Prescott JW. Quantitative imaging biomarkers: the application of advanced image processing and analysis to clinical and preclinical decision making. *J Digit Imaging.* 2013;26:97-108.

33. European Society of R. White paper on imaging biomarkers. *Insights Imaging.* 2010;1:42-45.

34. Koo HR, Moon WK, Chun IK, et al. Background (1)(8)F-FDG uptake in positron emission mammography (PEM): correlation with mammographic density and background parenchymal enhancement in breast MRI. *European journal of radiology.* 2013;82:1738-1742.

35. Vranjesevic D, Schiepers C, Silverman DH, et al. Relationship between 18F-FDG uptake and breast density in women with normal breast tissue. *Journal of nuclear medicine : official publication, Society of Nuclear Medicine.* 2003;44:1238-1242.

36. Kumar R, Chauhan A, Zhuang H, Chandra P, Schnall M, Alavi A. Standardized uptake values of normal breast tissue with 2-deoxy-2-[F-18]fluoro-D: -glucose positron emission tomography: variations with age, breast density, and menopausal status. *Mol Imaging Biol.* 2006;8:355-362.

37. Mavi A, Cermik TF, Urhan M, et al. The effect of age, menopausal state, and breast density on (18)F-FDG uptake in normal glandular breast tissue. *J Nucl Med.* 2010;51:347-352.

38. Muller-Schimpfle M, Ohmenhauser K, Stoll P, Dietz K, Claussen CD. Menstrual cycle and age: influence on parenchymal contrast medium enhancement in MR imaging of the breast. *Radiology.* 1997;203:145-149.

39. Carney PA, Miglioretti DL, Yankaskas BC, et al. Individual and combined effects of age, breast density, and hormone replacement therapy use on

the accuracy of screening mammography. *Ann Intern Med.* 2003;138:168-175.

40. Kelemen LE, Pankratz VS, Sellers TA, et al. Age-specific trends in mammographic density: the Minnesota Breast Cancer Family Study. *Am J Epidemiol.* 2008;167:1027-1036.

41. Melsaether A, McDermott M, Gupta D, Pysarenko K, Shaylor SD, Moy L. Inter- and intrareader agreement for categorization of background parenchymal enhancement at baseline and after training. *AJR American journal of roentgenology.* 2014;203:209-215.

42. Ciatto S, Houssami N, Apruzzese A, et al. Categorizing breast mammographic density: intra- and interobserver reproducibility of BI-RADS density categories. *Breast.* 2005;14:269-275.

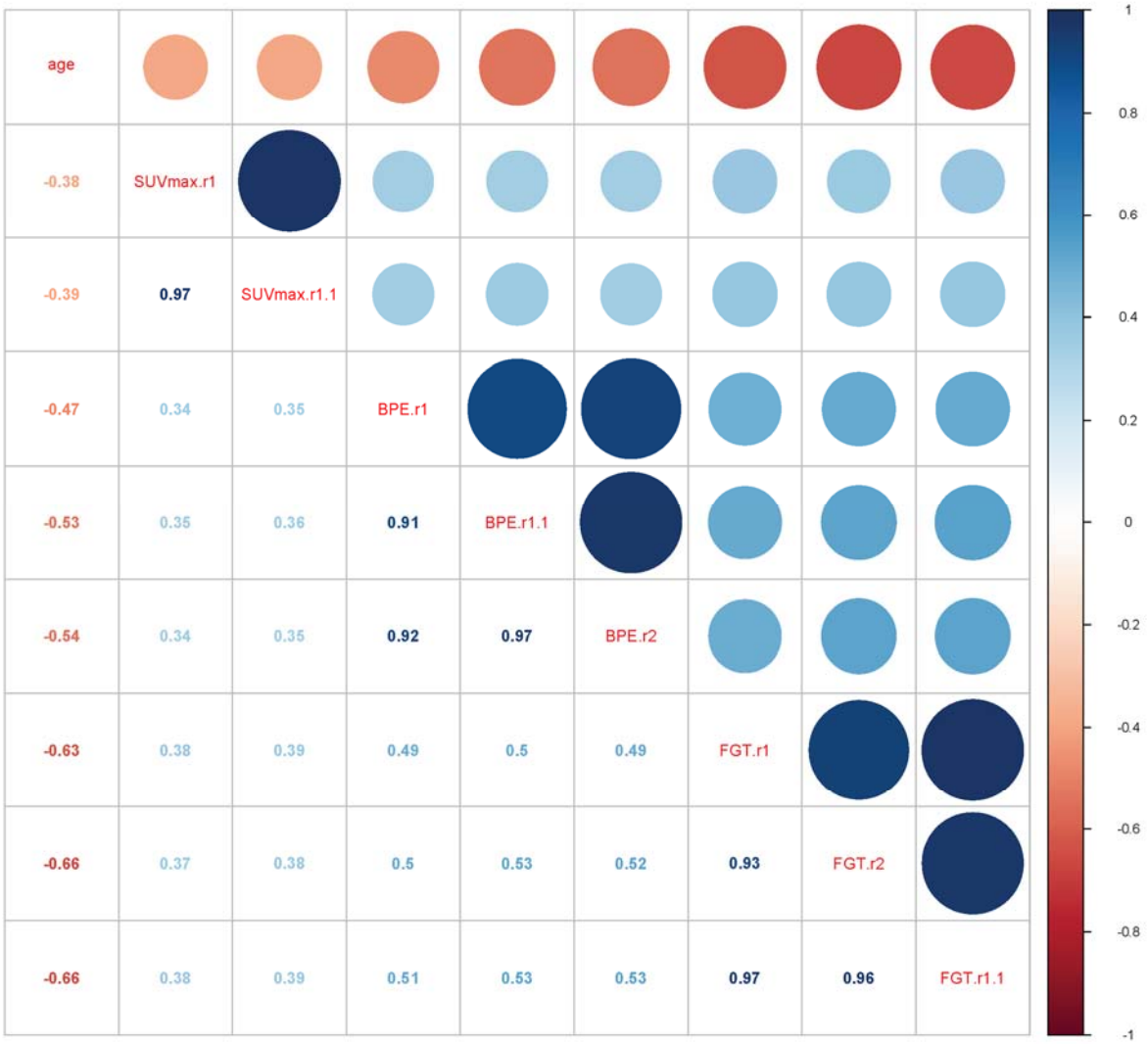

Figure 1

Correlation coefficient matrix showing numerical, color- and size-coded Spearman rank correlation coefficients for BPU SUVmax values in 18F-FDG PET/CT, BPE, FGT and age for both readers and reassessment of BPU

SUVmax values by reader 1. Correlations ranged from moderate to strong and are marked in blue if positive and red if negative (cf. legend on the right).

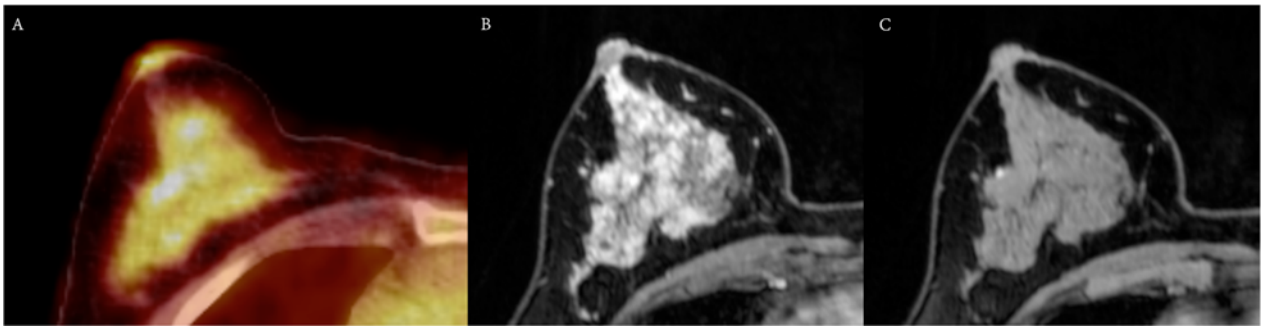

Figure 2

Fifty-four year-old woman presenting with a BPU SUVmax of 2.96 on 18F-FDG PET/CT showed marked BPE and extreme fibroglandular breast tissue (FGT-ACR D).

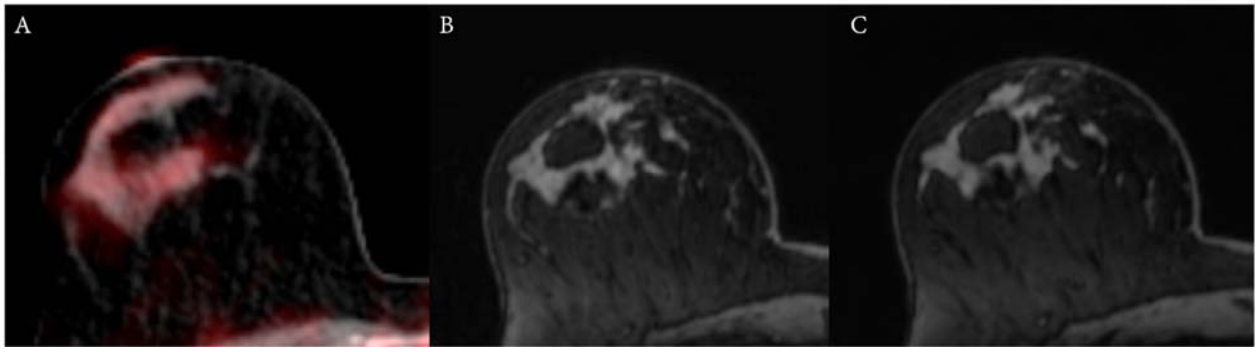

Figure 3

Sixty-one year-old woman presenting with a BPU SUVmax of 1.12 on 18F-FDG PET/CT showed no BPE and scattered fibroglandular breast tissue (FGT-ACR B).

Table 1:

Detailed results for ACR classification of BPE and FGT for both readers and reading rounds (r1_1; r1_2,; r2)

	r1	r1.1	r2
BPE			
minimal	58	61	60
mild	54	52	53
moderate	14	11	13
marked	3	5	3
FGT			
ACR a- almost entirely fatty	33	32	30
ACR b- scattered fibroglandular tissue	59	61	63
ACR c- heterogeneous fibroglandular tissue	27	24	22
ACR d- extreme fibroglandular tissue	10	12	14

Note: r1= reader 1; r1.1= reassessment by reader 1; r2= reader 2; BPE= background parenchymal enhancement; FGT= amount of fibroglandular tissue